

This item was submitted to [Loughborough's Research Repository](#) by the author.
Items in Figshare are protected by copyright, with all rights reserved, unless otherwise indicated.

Spike train dynamics underlying pattern formation in integrate-and-fire oscillator networks

PLEASE CITE THE PUBLISHED VERSION

PUBLISHER

© American Physical Society

LICENCE

CC BY-NC-ND 4.0

REPOSITORY RECORD

Bressloff, P.C., and S. Coombes. 2019. "Spike Train Dynamics Underlying Pattern Formation in Integrate-and-fire Oscillator Networks". figshare. <https://hdl.handle.net/2134/1732>.

Spike Train Dynamics Underlying Pattern Formation in Integrate-and-Fire Oscillator Networks

P. C. Bressloff and S. Coombes

*Nonlinear and Complex Systems Group, Department of Mathematical Sciences, Loughborough University,
Loughborough, Leicestershire LE11 3TU, United Kingdom*

(Received 9 April 1998)

A dynamical mechanism underlying pattern formation in a spatially extended network of integrate-and-fire oscillators with synaptic interactions is identified. It is shown how in the strong coupling regime the network undergoes a discrete Turing-Hopf bifurcation of the firing times from a synchronous state to a state with periodic or quasiperiodic variations of the interspike intervals on closed orbits. The separation of these orbits in phase space results in a spatially periodic pattern of mean firing rate across the network that is modulated by deterministic fluctuations of the instantaneous firing rate. [S0031-9007(98)07173-7]

PACS numbers: 87.10.+e, 05.45.+b

There has been much recent interest in studying the dynamics of pulse-coupled *integrate-and-fire* (IF) oscillators with applications to a wide range of systems including flashing fireflies [1], cardiac pacemaker cells [2], biological neural networks [3–10], digital phase-locked loops [11], and stick-slip models [12,13]. Most of the work has been concerned with the existence and stability of phase-locked solutions in which all oscillators have the same common frequency. A less well understood aspect of IF oscillators concerns the dynamics of more complex firing patterns. A number of studies of two-dimensional IF networks have shown that spontaneous excitations can occur leading to the formation of synchronized waves of activity across the network [14–17]. The analysis of pattern formation in such networks has so far been restricted to formulations in which the output of each oscillator is taken to be a mean firing rate [18]. This leads to an analog network model that is well known to undergo a Turing-like instability when there is competition between short-range excitation and long-range inhibition [19]. However, the mean-rate description does not include any information concerning the dynamics on short time scales. It is likely that the latter plays a significant role in the metastability of patterns, as has been illustrated by Usher *et al.* [18] in the case of noise-induced instabilities. Therefore, it is important to understand the basic mechanism of pattern formation in terms of the original spiking model without recourse to any mean-rate approximation.

In this Letter we analyze pattern formation in a spatially extended network of pulse-coupled IF oscillators with synaptic interactions. We begin by deriving conditions for the oscillators to be synchronized. We then determine the local stability of the synchronous state by considering perturbations of the oscillator firing times. We show how the synchronous state can undergo a discrete Turing-Hopf bifurcation of the firing times to a state with periodic or quasiperiodic variations in the interspike interval. The resulting spatiotemporal modulation of the oscillator firing

times leads to a spatially regular pattern of network output activity whose time-averaged properties are consistent with the behavior found in an analog version of the model.

Consider a d -dimensional network of IF oscillators. Let $U(\mathbf{x}, t)$ denote the state variable of the oscillator located at $\mathbf{x} \in \mathbb{R}^d$ at time t . Suppose that $U(\mathbf{x}, t)$ satisfies the equation

$$\frac{\partial U(\mathbf{x}, t)}{\partial t} = I_0 - U(\mathbf{x}, t) + g \int_{\mathbb{R}^d} W(|\mathbf{x} - \mathbf{x}'|) \hat{E}(\mathbf{x}', t) d\mathbf{x}' \quad (1)$$

supplemented by the reset condition $U(\mathbf{x}, t^+) = 0$ whenever $U(\mathbf{x}, t) = 1$. Here $\hat{E}(\mathbf{x}, t)$ represents the input from the oscillator at \mathbf{x} and I_0 is an external input that is taken to be time independent and homogeneous. The strength of the interactions between oscillators is determined by the coupling parameter g , $g > 0$, and the pattern of connectivity is specified by the weight function $W(|\mathbf{x}|)$ where $|\mathbf{x}| = \sqrt{\sum_{i=1}^d x_i^2}$. We shall assume that $I_0 > 1$ so that in the absence of any coupling, $g = 0$, each oscillator fires at a rate $1/T_0$ with $T_0 = \ln[I_0/(I_0 - 1)]$. Neglecting the shape of an individual pulse, the output spike train of each oscillator is represented as a sequence of Dirac delta functions, $E(\mathbf{x}, t) = \sum_{j=-\infty}^{\infty} \delta(t - T_j(\mathbf{x}))$, where $T_j(\mathbf{x})$ is the j th firing time of the oscillator at \mathbf{x} , that is, $U(\mathbf{x}, T_j(\mathbf{x})) = 1$ for all integers j . Each spike is converted to a postsynaptic potential whose shape is given by the so-called α function $J(\tau) = \alpha^2 \tau e^{-\alpha\tau}$ so that $\hat{E}(\mathbf{x}, t) = \int_0^{\infty} J(\tau) E(\mathbf{x}, t - \tau) d\tau$. [One could also include other features such as axonal transmission delays and dendritic delays into the definition of the delay kernel $J(\tau)$.] Finally, we shall take the weight distribution to be the difference of Gaussians $W(r) = W_1(r) - W_2(r)$, $W_i(r) = A_i e^{-r^2/2\sigma_i^2} / (\sqrt{2\pi} \sigma_i)^d$, with $\sigma_1 < \sigma_2$ and $A_1 \sigma_2^d > A_2 \sigma_1^d$. This combination of short-range excitation and long-range inhibition is the most common

form of architecture used to model pattern formation in neural systems. It will be convenient for our subsequent analysis to set $A_1 = A_2 = 1$ so that there is an equal balance between excitation and inhibition, that is, $\bar{W} \equiv \int_0^\infty r^{d-1} W(r) dr = 0$. (This condition is not necessary, however, for pattern formation to occur.)

At least in the case of slow synapses (small α), the IF model can be reduced to a mean firing-rate (analog) model since incoming spike trains are sampled over a relatively long time interval. This leads to the following integral equation for the averaged current $I(\mathbf{x}, t)$:

$$I(\mathbf{x}, t) = g \int_{\mathbb{R}^d} W(|\mathbf{x} - \mathbf{x}'|) \times \int_0^\infty J(\tau) f(I(\mathbf{x}', t - \tau)) d\tau d\mathbf{x}', \quad (2)$$

where $f(I) = \{T_{\text{ref}} + \ln[\frac{I_0 + I}{I_0 + I - 1}]\}^{-1}$ is the mean firing rate and T_{ref} is the absolute refractory period between pulses. Since $\bar{W} = 0$, it is clear that $I(\mathbf{x}, t) = 0$ for all \mathbf{x} and t is a solution of Eq. (2). Linearizing Eq. (2) about this zero solution and setting $I(\mathbf{x}, t) = I_0 e^{i\mathbf{p} \cdot \mathbf{x} + \lambda t}$ leads to the characteristic equation

$$\left(1 + \frac{\lambda}{\alpha}\right)^2 = g f'(0) \tilde{W}(p), \quad (3)$$

where $\tilde{W}(p) = e^{-p^2 \sigma_1^2 / 2} - e^{-p^2 \sigma_2^2 / 2}$ is the Fourier transform of $W(r)$ and $p^2 = \sum_{i=1}^d p_i^2$. It is then easy to establish that the zero homogeneous state undergoes a Turing-like instability [19] at a critical value of the coupling where $1 = g_c f'(0) \tilde{W}(p_c)$ and $\tilde{W}(p_c) = \max_p \tilde{W}(p)$, that is, $p_c^2 = 4 \ln(\sigma_2 / \sigma_1) / (\sigma_2^2 - \sigma_1^2)$. Depending on the initial conditions, one finds that beyond the bifurcation point large-scale spatial patterns develop whose wavelength close to the bifurcation point is approximately $2\pi / p_c$.

We shall now investigate the analogous mechanism for pattern formation in the original IF model of Eq. (1). We begin by restricting our attention to phase-locked solutions of Eq. (1) in which every oscillator resets or fires with the same self-consistent period T . (Such solutions play an analogous role to the homogeneous zero solution in the mean-rate model.) The state of each oscillator can then be characterized by a constant phase $\phi(\mathbf{x}) \in \mathbb{R} \setminus \mathbb{Z}$ such that the j th firing time of the oscillator at \mathbf{x} is $T_j(\mathbf{x}) = [j - \phi(\mathbf{x})]T$, integer j . We can now integrate Eq. (1) over the interval $t \in [-T\phi(\mathbf{x}), T - T\phi(\mathbf{x})]$ and incorporate the reset condition by setting $U[\mathbf{x}, -\phi(\mathbf{x})T] = 0$ and $U[\mathbf{x}, T - \phi(\mathbf{x})T] = 1$. This leads to the set of integral equations

$$1 = (1 - e^{-T})I_0 + g \int_{\mathbb{R}^d} W(|\mathbf{x} - \mathbf{x}'|) \times K_T[\phi(\mathbf{x}') - \phi(\mathbf{x})] d\mathbf{x}', \quad (4)$$

where $K_T(\phi) = e^{-T} \int_0^T e^t \hat{J}_T(t + \phi T) dt$ and $\hat{J}_T(t)$ is a T -periodic function of t with $\hat{J}_T(t) = \sum_{j=0}^\infty J(t + jT)$ for

$0 \leq t < T$. The periodic interaction function $K_T(\phi)$ can be evaluated explicitly when $J(\tau)$ is an α function since $\hat{J}_T(t)$ reduces to a geometric series. For more general delay kernels one can use Fourier series to determine $K_T(\phi)$. After choosing some reference oscillator, Eq. (4) determines the relative phases and the period T of the phase-locked state.

One class of phase-locked solutions of Eq. (4) is guaranteed to exist by the translational symmetry of the system, namely, rotating waves of the form $\phi(\mathbf{x}) = \mathbf{k} \cdot \mathbf{x} + \phi_0$ where \mathbf{k} is a wave vector and ϕ_0 is an arbitrary constant (which we shall set to zero). The particular solution with $\mathbf{k} = 0$ corresponds to the synchronous state. Substitution into Eq. (4) leads to a single independent equation that determines a dispersion relation for the collective period, $T = T(\mathbf{k})$. It is important to realize that the rotating wave solutions involve spatial modulations in the firing phase of the oscillators under the assumption that there is 1:1 frequency locking. However, the distribution of network output activity across the network, as specified by the interspike intervals $\Delta_j(\mathbf{x}) = T_{j+1}(\mathbf{x}) - T_j(\mathbf{x})$, is homogeneous since $\Delta_j(\mathbf{x}) = T$ for all $j \in \mathbb{Z}$, $\mathbf{x} \in \mathbb{R}^d$. We shall establish in this Letter that a phase-locked homogeneous state can undergo a *discrete Turing-Hopf* instability of the firing times to a state in which there is a spatial variation in the average firing rate of the oscillators across the network. In the case of a one-dimensional network we show that the resulting patterns are consistent with those generated via a *Turing* instability in mean firing rate of the analog version described by Eq. (2).

The linear stability of a phase-locked solution of Eq. (4) can be determined by considering perturbations of the firing times $T_j(\mathbf{x}) = [j - \phi(\mathbf{x})]T + \delta_j(\mathbf{x})$. This method was previously used by van Vreeswijk to study globally coupled IF networks [20]. In order for the analysis to be tractable, we shall concentrate on the stability of the synchronous state $\phi(\mathbf{x}) = 0$ for all \mathbf{x} . Thus we take $T_j(\mathbf{x}) = jT + \delta_j(\mathbf{x})$ and integrate Eq. (1) from $T_j(\mathbf{x})$ to $T_{j+1}(\mathbf{x})$ using the reset condition. If the resulting equation is expanded as a power series in the perturbations δ then to $\mathcal{O}(1)$ we recover Eq. (4) for the synchronous state. Under the simplifying condition $\bar{W} = 0$, this reduces to $1 = (1 - e^{-T})I_0$, that is, $T = T_0$. The $\mathcal{O}(\delta)$ term leads to a linear delay-difference equation for the perturbations $\delta_k(\mathbf{x})$ which, after substitution of the solution $\delta_k(\mathbf{x}) = e^{k\lambda + i\mathbf{p} \cdot \mathbf{x}}$, yields the characteristic equation [21]

$$(e^\lambda - 1)[I_0 - 1] = g \tilde{W}(p) G(\lambda, T_0) \quad (5)$$

with $\lambda \in \mathbb{C}$, $0 \leq \text{Im } \lambda < 2\pi$, and

$$G(\lambda, T) = \frac{\alpha^2 e^{-T} [(1 - \alpha T + \alpha^2 T) e^{(1-\alpha)T} - 1]}{(1 - e^{-\alpha T - \lambda})(1 - \alpha)^2} - \frac{T \alpha^3 e^{-T} e^{-\alpha T - \lambda} [e^{(1-\alpha)T} - 1]}{(1 - e^{-\alpha T - \lambda})^2 (1 - \alpha)}. \quad (6)$$

Note that the function $G(\lambda, T)$ has a pole at $\lambda = -\alpha T$. Solutions of the characteristic Eq. (5) determine a dispersion relation $\lambda = \lambda(p)$. The invariance of the dynamics with respect to uniform shifts in the firing times, $T_j(\mathbf{x}) \rightarrow T_j(\mathbf{x}) + \delta$, is reflected by the identity $\lambda(0) = 0$. Thus the condition for linear stability of the synchronous state is $\text{Re } \lambda(p) < 0$ for all $p \neq 0$.

For sufficiently small coupling, solutions to Eq. (5) in the complex λ plane will be either in a neighborhood of the real solution $\lambda = 0$ or in a neighborhood of the pole at $\lambda = -\alpha T$. Since the latter has a negative real part, the stability of the phase-locked solution will be determined by the eigenvalues close to the origin. To first order in g we can set $\lambda = 0$ on the right-hand side of Eq. (5) so that the spectrum close to the origin is determined by the equation $\lambda(I_0 - 1) = g\tilde{W}(p)G(0, T_0) + \mathcal{O}(g^2)$. One finds that $G(0, T_0) < 0$ for all α . Hence, the synchronous state is stable since $\tilde{W}(p) > 0$ for all $p \neq 0$. It is also easy to establish that the synchronous state cannot undergo a static bifurcation (with one or more real eigenvalues crossing the origin) into another phase-locked solution as g increases. (For convenience, we restrict ourselves in this Letter to solutions that are spatially periodic so that the spectrum associated with Eq. (3) or (5) is discrete.)

However, it is possible for the synchronous state to undergo a Hopf bifurcation to a state with periodic or quasiperiodic interspike intervals due to a complex conjugate pair of eigenvalues crossing the imaginary axis. Substituting $\lambda = i\omega$, $\omega \neq 0$ into Eq. (5) and equating real and imaginary parts leads to the pair of simultaneous equations

$$H_0(\omega, \hat{g}) \equiv [\cos(\omega) - 1](I_0 - 1) - \hat{g}C(\omega) = 0, \quad (7)$$

$$H_1(\omega, \hat{g}) \equiv \sin(\omega)(I_0 - 1) + \hat{g}S(\omega) = 0, \quad (8)$$

where $\hat{g} = g\tilde{W}(p)$ and $C(\omega) = \text{Re } G(i\omega, T_0)$, $S(\omega) = -\text{Im } G(i\omega, T_0)$. The latter can be calculated explicitly using Eq. (6) [21]. We find that for all α there exists

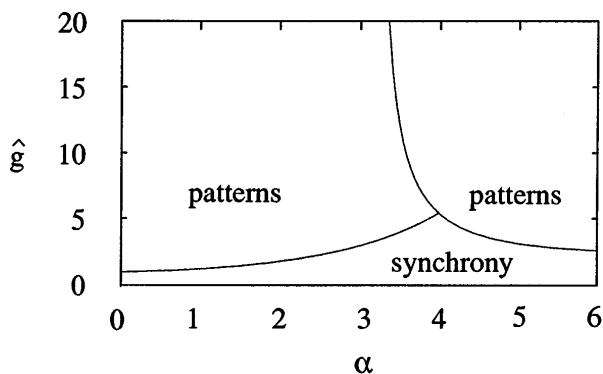


FIG. 1. The solutions of Eqs. (7) and (8) for \hat{g} are plotted as a function of α with $I_0 = 1.5$. For a given α , the branch with the smallest \hat{g} determines the critical coupling \hat{g}_c for desynchronization via a Turing-Hopf bifurcation in the firing times.

at least one solution (ω, \hat{g}) to Eqs. (7) and (8). The positive solution branches for \hat{g} are plotted as a function of the inverse rise time α in Fig. 1. It follows that a Hopf bifurcation in the firing times occurs at a critical coupling strength g_c such that $g_c\tilde{W}(p_c) = \hat{g}_c$, where \hat{g}_c is the smallest solution for \hat{g} and $\tilde{W}(p_c) = \max_p \tilde{W}(p)$. Since $p_c \neq 0$, the instability will involve spatially inhomogeneous perturbations with wave vectors satisfying $\mathbf{p}^2 \approx p_c^2$. Hence, the firing times can be said to undergo a discrete *Turing-Hopf* instability.

The occurrence of such an instability leads to the creation of closed periodic or quasiperiodic orbits (invariant circles) for the interspike intervals. We denote these invariant circles by $\mathcal{M}(\mathbf{x})$. Define the long-term average firing rate according to $a(\mathbf{x}) = \bar{\Delta}(\mathbf{x})^{-1}$ where $\bar{\Delta}(\mathbf{x}) = \lim_{M \rightarrow \infty} \sum_{j=-M}^M \Delta_j(\mathbf{x}) / (2M + 1)$. Then spatial (\mathbf{x} -dependent) variations in the firing rates $a(\mathbf{x})$ will occur if there is a corresponding spatial distribution of the invariant circles $\mathcal{M}(\mathbf{x})$ in phase space. This is illustrated in Figs. 2 and 3 for a one-dimensional ($d = 1$) network of IF oscillators just beyond the Turing-Hopf bifurcation point. Figure 2 shows that the invariant circles are separated from each other in phase space (although they remain small relative to the natural time scales of the system). The resulting long-term average behavior of the system is characterized by spatially regular patterns of output activity as shown in Fig. 3a. These patterns are found to be consistent with those observed in the analog version of the model, Eq. (2), and such agreement holds over a wide range of values of α that includes both fast and slow synapses. However, the IF model has additional fine structure associated with the dynamics on the

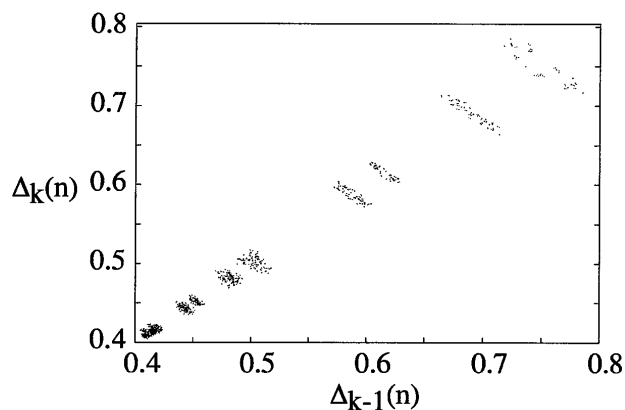


FIG. 2. Separation of the (projected) invariant circles in phase space for a 1D network of $N = 50$ IF oscillators (with periodic boundary conditions) close to a Hopf bifurcation point. The discretized interaction kernel is taken to be $W(n) = A \exp[-n^2/(2\sigma_1^2 N)] - B \exp[-n^2/(2\sigma_2^2 N)]$ for $n \neq 0$ with $A = (2\pi\sigma_1)^{-1}$ and B chosen so that $\sum_m W(m) = 0$. We also set $W(0) = 0$. The attractor of the embedded interspike interval (ISI) with coordinates, $(\Delta_{k-1}(n), \Delta_k(n))$, is shown for all N oscillators with $\alpha = 2$, $g = 0.4$, $I_0 = 1.5$, $\sigma_1 = 0.3$, and $\sigma_2 = 0.5$.

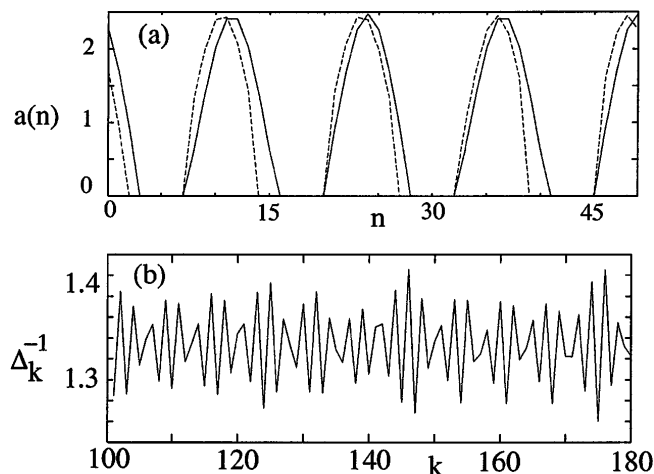


FIG. 3. (a) Regular spatial variations in the long-term average firing rate $a(n) = \bar{\Delta}(n)^{-1}$ for the IF network considered in Fig. 2 (dashed curve). There is good agreement with the corresponding patterns found in an analog version of the network (solid curve) in which $a(n) = f(I(n))$ with $T_{\text{ref}} = 0$. (b) Variation of inverse ISI $(\Delta_k)^{-1}$ of the oscillator $n = 1$ as a function of k .

invariant circles, which is not resolved by the analog model. This is illustrated in Fig. 3b where we plot temporal variations in the instantaneous firing rate of one of the oscillators shown in Fig. 3a. The relative size of the deterministic fluctuations in the mean firing rate is found to be an increasing function of α , approaching zero as $\alpha \rightarrow 0$.

In conclusion, we have identified a basic dynamical mechanism for pattern formation in IF oscillator networks. This involves desynchronization via a Turing-Hopf bifurcation to a state with periodic or quasiperiodic variations of the interspike intervals on invariant circles separated in phase space. We have also shown that in the case of one-dimensional networks such patterns are consistent with those of a corresponding analog model. Numerical results by Usher *et al.* [18] suggest that this result also holds for two-dimensional networks. A much more detailed analysis of two-dimensional networks will be presented elsewhere [21] where we shall also consider the more bio-

logically realistic case of two populations of IF oscillators, one excitatory with short-range interactions and the other inhibitory with long-range interactions.

This research was supported by Grant No. GR/K86220 from the EPSRC (U.K.).

-
- [1] R. E. Mirollo and S. H. Strogatz, *SIAM J. Appl. Math.* **50**, 1645 (1990).
 - [2] C. Peskin, *Mathematical Aspects of Heart Physiology* (Courant Institute of Mathematical Sciences, New York University, New York, 1975).
 - [3] Y. Kuramoto, *Physica (Amsterdam)* **50D**, 15 (1991).
 - [4] L. F. Abbott and C. van Vreeswijk, *Phys. Rev. E* **48**, 1483 (1993).
 - [5] M. V. Tsodyks, I. Mitkov, and H. Sompolinsky, *Phys. Rev. Lett.* **71**, 1280 (1993).
 - [6] C. van Vreeswijk, L. F. Abbott, and G. B. Ermentrout, *J. Comp. Neurosci.* **1**, 313 (1994).
 - [7] W. Gerstner, *Phys. Rev. E* **51**, 738 (1995).
 - [8] D. Hansel, G. Mato, and C. Meunier, *Neural Comput.* **7**, 307 (1995).
 - [9] S. Coombes and G. J. Lord, *Phys. Rev. E* **56**, 5809 (1997).
 - [10] P. C. Bressloff, S. Coombes, and B. de Souza, *Phys. Rev. Lett.* **79**, 2791 (1997).
 - [11] G. Goldsztein and S. H. Strogatz, *Int. J. Bifurcation Chaos* **5**, 983 (1994).
 - [12] S. Bottani, *Phys. Rev. Lett.* **74**, 4189 (1995).
 - [13] A. V. Herz and J. J. Hopfield, *Phys. Rev. Lett.* **75**, 1222 (1995).
 - [14] P. H. Chu, J. G. Milton, and J. D. Cowan, *Int. J. Bifurcation Chaos* **4**, 237 (1994).
 - [15] C. Fohlmeister, W. Gerstner, R. Ritz, and J. L. van Hemmen, *Neural Comput.* **7**, 905 (1995).
 - [16] D. Horn and I. Opper, *Neural Comput.* **9**, 1677 (1997).
 - [17] W. M. Kistler, R. Seitz, and J. L. van Hemmen, *Physica (Amsterdam)* **114D**, 273 (1998).
 - [18] M. Usher, M. Stemmler, and Z. Olami, *Phys. Rev. Lett.* **74**, 326 (1995).
 - [19] G. B. Ermentrout and J. D. Cowan, *Biol. Cybernet.* **34**, 137 (1979).
 - [20] C. van Vreeswijk, *Phys. Rev. E* **54**, 5522 (1996).
 - [21] P. C. Bressloff and S. Coombes (unpublished).